



Modelling vSGPs (very shallow geothermal potentials) in selected CSAs (case study areas)



D. Bertermann^a, H. Klug^{b,*}, L. Morper-Busch^b, C. Bialas^a

^aUniversity of Erlangen – Nuremberg, GeoZentrum Nordbayern, Schlossgarten 5, 91054 Erlangen, Germany

^bUniversity of Salzburg, Interfaculty Department of Geoinformatics, Schillerstr. 30, 5020 Salzburg, Austria

ARTICLE INFO

Article history:

Received 3 October 2013

Received in revised form

14 April 2014

Accepted 18 April 2014

Available online 15 May 2014

Keywords:

TC (thermal conductivity)

VHC (volumetric heat capacity)

Heat transfer

Spatial analysis

Particle-size fraction

Soil water content

ABSTRACT

Very shallow geothermal energy resources are amongst the RES (renewable energy sources). They can be expressed as TC (thermal conductivity) (W/m³*K) and VHC (volumetric heat capacity) (MJ/m³*K) of unconsolidated ground, and can be obtained from a depth of 10 m below the Earth's surface. Utilising horizontal and vertical heat collector systems, these geothermal energy sources can be harnessed for heating and cooling purposes of residential and industrial buildings. To ensure proper prediction of available potentials at landscape or even local scale, downscaling of the already existing pan-European vSGP (very shallow geothermal potential) at a scale of 1:250,000 is required. Therefore, we applied an advanced methodology to 14 European CSAs (case study areas) from which we selected two German and one Austrian area for demonstration purposes. To ensure comparability across CSAs, national and case study related datasets were standardised and harmonised. Standards and unified spatial data processing methods across CSAs ensure comparability and seamless visualisation. Laboratory investigations on TC demonstrate valid modelling results for three depth layers, visualised in a publicly available WebGIS.

© 2014 Elsevier Ltd. All rights reserved.

1. Introduction

Europe and many of its 27 member states are turning away from non-renewable nuclear, coal, and gas energy resources, and now foster alternative renewable energy resources as a response to climate change [1,2]. Amongst the renewable energy resources is the geothermal (heat) energy. This is CO₂-neutral, quasi-inexhaustible, and de-centrally available at any time and almost everywhere for sustainable heating and cooling of residential and industrial buildings [3–6]. The underground's naturally given solar energy storage for heating and cooling of housings as such is not new. In the past, heat collected by solar panels was transferred and stored to the underground [7–10]. An overview of underground long-term storage of solar energy was already provided by Shelton [11] and Givoni [12], while the behaviour of the thermal energy storage in the ground was modelled by Reuss et al. [13].

Much research has been conducted in shallow (<400 m depth) and deep (>400 m depth) geothermal energy potentials, but Bertermann et al. [14] were the first who provided a pan-European

overview of the vSGP (very shallow geothermal potential) directly below the surface. This map is intended to provide a decision support tool for energy policies on a European to national scale, and thereby serves to contribute NREAPs (National Renewable Energy Action Plans) to the RES (Renewable Energy Sources) [15]. To ensure improved estimation results at a landscape to local scale, both the quality of digitally available and accessible spatial datasets and the application of the preferred methodology need to be adapted, improved and harmonised accordingly.

Soil heat and soil moisture processes are interconnected when the heat transport is facilitated through infiltrating water [16–18]. While the TC (thermal conductivity) reflects the ability of soil and soft rock material to direct heat to the underground, the VHC (volumetric heat capacity) describes the ability of a given soil and soft rock volume to store internal energy while undergoing a given temperature change [19,20]. In other words, VHC shows the amount of solar driven heat required to change the temperature of the soil matrix. Since the VHC of the soil is directly proportional to its volume, BD (bulk density) is an important parameter [18,21].

Physical soil properties including hydraulic characteristics are immediately linked to the soil structure given by the pore space and its respective spatial distribution. Characterising water processes at the local scale requires an accurate and high-resolution description

* Corresponding author. Tel.: +43 662 8044 7561.

E-mail addresses: Hermann.Klug@sbg.ac.at, office@hermannklug.com (H. Klug).

of the variability of representative state variables [22]. Pedotransfer functions can be used for estimating the spatial distribution of physical soil properties. Relating soil structural features of porous media to their functional properties still remains a scientific challenge [23]. Point-based spatially enabled soil property databases [24,25], or estimation and interpolation methods of physical soil properties exist [26]. Pedotransfer functions are also available to estimate the permeability and compaction characteristics of soils [27], and the distribution of a three dimensional soil pore space [28]. However, soil sampling is also required to validate the digitally available soil maps [29]. Moreira et al. [30] investigate the ability of laboratory methods to predict soil BD and compare its performance with published pedotransfer functions. Knowledge of water percolation and conductivity is essential for studying water, and thus heat transport in soil, but the study done by Touma [31] shows that different approaches provide different results; however, he concluded that “the hydraulic conductivity of a soil can be predicted from its water retention”. Thus, based on the hydrologic conditions and the soil temperature, the TC of soils can be determined by the temperature in different soil depths [32,33].

The hydrological conditions can be described by humidity indices [34] using precipitation and temperature datasets for calculation. Existing gridded (regional) air temperature and precipitation products can be used for the calculation of the humidity index [35–37].

Annual air temperature values can also be used to estimate the average soil temperature at different depths, and it can be estimated for any time and location on the basis of its annual periodicity [5,38–40]. Furthermore, there exist many modelling approaches to estimate the soil surface temperature [41,42]. The overall dependence of solar radiation, the respective soil temperature, the given soil water content at various depths, and the resulting soil surface heat flux were underpinned by an experimental run conducted by Balghouthi et al. [43].

Our contribution in this paper is based on an integrated assessment [44], interlinking the domains of climatology, pedology and hydrology, and is contributing to the PRES (“Process Integration, Modelling and Optimisation for Energy Saving and Pollution Reduction”) [45]. Our main objective is to tailor the approach of the EOM (European Outline Map) available in 1:250,000 to CSA (case study area) maps in meso to local scale. To estimate the vSGP we provide an advanced methodology after Bertermann et al. [14], calculating the TC in W/m^2K and the VHC in MJ/m^3K . We selected 14 CSAs within nine European countries, using national or even local datasets available, and validated our approach with laboratory investigations. We hypothesise that spatial datasets available in national repositories or CSAs are appropriate for examining the vSGP on a local to landscape scale. We additionally hypothesise that these datasets can be technically and semantically harmonised to provide a seamless and comparable view across CSAs and that modelling results are amenable to laboratory findings.

2. Materials and methods

2.1. CSAs and datasets

In the EC co-funded ThermoMap project, a total of 14 CSAs has been developed, from which three were selected for demonstration in this manuscript, namely, the Mondsee catchment in Austria (246 km²), and the two German case studies Büchenbach (2.5 km²) and Röttenbach (0.04 km²) (Fig. 1, Table 1). These CSAs were chosen to represent the different scales from 1:5000 to 1:50,000. Thus, the size of the CSAs and resolution of the datasets used herein have been selected flexibly to account for variations in data quality and quantity. This flexibility ensures that individual datasets could be

used most appropriately, [22], and a transfer of the methodology to other areas is assured.

2.2. The Mondsee CSA, Austria

The catchment area of Lake Mondsee is about 5 km east of the capital of the Federal State of Salzburg, Austria, and has an area of 246 km². The grassland dominated landscape with meadows, amongst them forests, comprises about a dozen medium-sized lakes (plus a large number of small ones), embedded in a landscape of Flysch hills in the northern and western parts, and Alpine calcareous mountains in the southern and eastern parts. The landscape ranges between an altitude of 413 and 1780 masl, and has an annual average precipitation rate of 1395 mm and an annual average temperature of 8 °C. According to Table 2, very detailed spatial datasets are available and have been used in this study.

2.3. The Büchenbach CSA, Germany

The German test site Büchenbach is located in the west of Erlangen between the districts Büchenbach (north/east), Steudach (south), Häusling (west) and Kosbach (northwest). It comprises a mostly flat rural area, traversed by small rivulets and pond strings in west–east-direction. The area is 2.5 km² [in extent] and is largely used for agricultural production. The climatic conditions are continental and therefore relatively warm and dry. Topographically, the test area is located at an altitude between 290 and 320 masl. Geologically it is located within the Franco-Swabian escarpment region (so-called “Keuper-Lias-Land”/Germanic Triassic period). Soil types are Cambisols, Regosols, Pelosols, Gleysols, and Planosols with soil textures dominated by clay and loam. Büchenbach is a developing district of Erlangen. New building constructions here are planned to have heat supplied from renewable energy resources.

2.4. The Röttenbach CSA, Germany

The second German test site is located at the north-western edge of the town Röttenbach, around 7 km north–west of the city Erlangen. The CSA, 4 ha in size, is presently under agricultural production. The climate is continental and thus warm and dry with an annual precipitation rate of approximately 600 mm. This slightly sloping area is declared to become a new development district with a dedicated geothermal heat and energy supply system. Similar to the previous test site, the altitude ranges between 310 and 320 masl and is likewise geologically structured. Cambisols with a loamy to rather sandy soil texture have been observed for most parts of the area. Datasets used for the two German CSAs are listed in Table 3.

2.5. The local- to meso-scale vSGP modelling methodology

2.5.1. General considerations

The vSGP for the CSA considers a four step approach. While the inner circle in Fig. 2 highlights the procedure of the EOM, the outer circle highlights the methodological advancements applied for the CSA approach. In general, all procedures from the inner circle remain the same in the CSA; however, datasets used are dissimilar. Thus, only the advanced modelling steps are highlighted in the outer circle of Fig. 2.

The CSA approach extends the analysis from the maximum of 3 m in the EOM to 10 m below surface in the CSA. These 10 m have been subdivided into three main layers:

- 0–3 m (first),
- 3–6 m (second), and

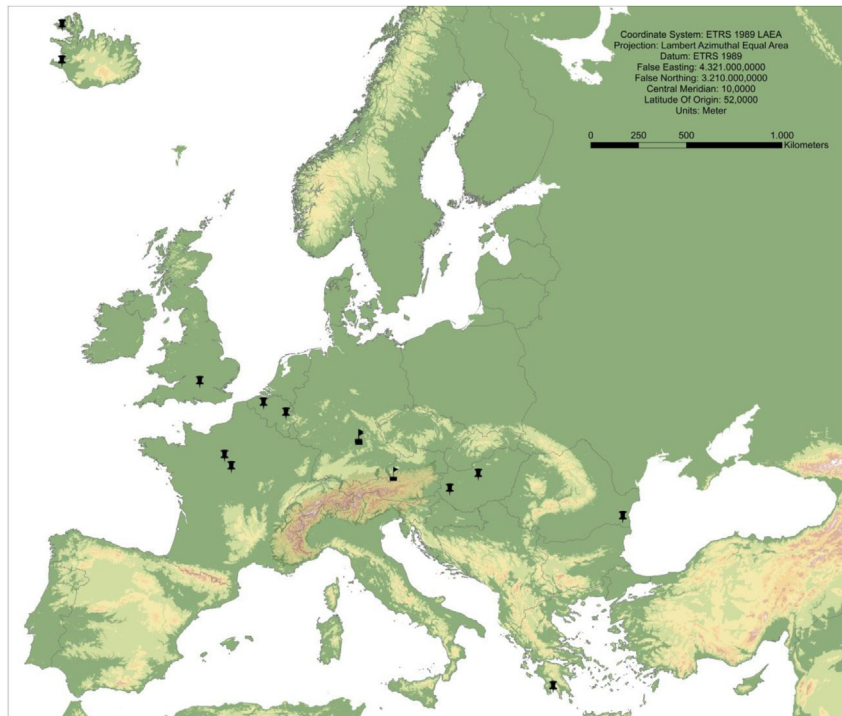


Fig. 1. The locations of the project related case studies (push pins) and case studies selected in this manuscript (flags).

■ 6–10 m (third).

These depth layers consider the usual installation depth of the different horizontal (slinky and trench collectors) and vertical (helix and basket collectors) heat collector technologies available to date. Thus, soil texture analysis (considered in step 3), TC modelling and VHC modelling (considered in step 4) are processed separately for each depth layer. This is valid until exclusion criteria such as consolidated ground apply (see step 1).

The identification of unconsolidated soil depth (zone of soft rock) was not possible within the EOM. Within the CSA approach we could distinguish the depth of the unconsolidated ground and the respective soil texture information according to the following procedure:

1. Soil property attributes have been extracted from available soil and geological maps. If drilling information was available, it was

Table 1
CSAs (case study areas).

Country	Name	Size (km ²)
<i>Austria</i>	<i>Mondsee catchment</i>	246
<i>Belgium</i>	<i>City of Gent</i>	1600
<i>Belgium</i>	<i>City of Liège</i>	600
<i>France</i>	<i>Agglomeration of Orléans</i>	334
<i>France</i>	<i>Eure-et-Loir department</i>	5880
<i>Germany</i>	<i>Büchenbach</i>	2.5
<i>Germany</i>	<i>Röttenbach</i>	0.04
<i>Greece</i>	<i>City of Kalamata</i>	72
<i>Hungary</i>	<i>Budapest</i>	113
<i>Hungary</i>	<i>Zalakoppány</i>	34.8
<i>Iceland</i>	<i>Mosfellssveit-Kjalarnes</i>	120
<i>Iceland</i>	<i>Otradalur</i>	20
<i>Romania</i>	<i>Constanta</i>	7100
<i>United Kingdom</i>	<i>Drayton St Leonard</i>	25

The CSAs (case study areas) presented in this manuscript appear in italics.

included. For the estimation of the depth of the unconsolidated ground and respectively the estimation of the dominating soil texture within the first layer (0–3 m), information on the soil type has additionally been considered.

2. For the second layer (3–6 m) and the third layer (6–10 m), stratum information was extracted from Quaternary (geological) maps. Weathering characteristics have been taken into account for soil texture and soil depth estimation. In case of lacking Quaternary information, the respective bedrock (parent rock) and its weathering characteristics were used.
3. Within the TMMV (ThermoMap MapViewer), the hatchings in the second and third layers indicate areas where the depth is not completely available for installations due to soft rock zone limitations.

Despite the mentioned changes from the EOM to this advanced methodology at CSA level, the time scale of providing annual average information of the TC did not change.

2.5.2. Step 1: Exclusion criteria and limiting factors

Exclusion criteria: Areas with a soft rock thickness of less than 3 m, as well as permafrost, and water bodies are considered as unattractive, respectively, unusable for the installation of very shallow geothermal energy systems for technical and economic reasons.

Limiting factors: Limitations are considered as areas where certain spatial properties limit the installation of very shallow geothermal energy systems. These areas are not excluded from the potential estimation, but the geothermal usage could require additional clarifications. Protection areas for instance usually have legal restrictions which apply to modifications of the underground. Since there is no explicit and uniform definition of a protected area valid for each European member state, the datasets used at CSA level are case dependent. For each CSA, independent decisions on protection zones apply. Zones for instance include regions for

Table 2
The Mondsee catchment datasets.

Parameter group	Parameter/Dataset description	Unit(s)	Scale/Resolution Accuracy of the dataset	File format/Projection	Data source(s)	Remarks and further information
Climate conditions	Annual and monthly average total precipitation	mm/month mm/year	Scale: 1:25,000–1:50,000 Resolution: 90 m × 90 m	Shapefile/WGS 84	Climate station datasets from: ■ Austrian Environmental Agency (BMLFUW) ■ Hydrological Surveys Salzburg and Upper Austria ■ ZAMG (Austrian Central Institute for Meteorology and Geodynamics)	■ Processing: interpolation and vectorisation ■ Datasets are classified into 5 mm increments, legend is classified into 100 mm increments
Climate conditions	Annual mean and monthly air temperature	°C	Scale: 1:25,000–1:50,000 Resolution: 90 m × 90 m	Shapefile/WGS 84	Climate station datasets from: ■ Austrian Environmental Agency (BMLFUW) ■ Hydrological Surveys Salzburg and Upper Austria ■ ZAMG (Austrian Central Institute for Meteorology and Geodynamics)	■ Processing: interpolation and vectorisation ■ Datasets are classified into 0.5 °C increments, legend is classified into 1 °C increments
Topographical and hydro-/geological parameters	Slope	° [degree]	Resolution: 10 m × 10 m	Shapefile/WGS 84	DEM from Austrian Federal Office for Meteorology and Survey (Bundesamt für Eich- und Vermessungswesen)	Processing: DEM to slope and classification in 5° increments
Topographical and hydro-/geological parameters	Depth of the (ground) water table	Meters below surface [m]	1:1 Mio.	Shapefile/WGS 84	Hydrological Atlas of Austria (HAÖ)	Estimation is based on hydrological and hydrogeological maps
Topographical and hydro-/geological parameters	Depth of the soft rock zone/Indication of the thickness	Meters below surface [m]	1:50,000 (Geology) 1:1,500,000. (Lithology)	Raster/Vector (Geology) shapefile/WGS 84 (Lithology)	■ Austrian soil map (ÖBK sheets 48, 49, 72, 79, 91, 108) ■ Geological Survey of Austria: Geological maps of the test area (GÖK 64 Thalgau & GÖK 65 Mondsee) ■ Austrian Bedrock Lithology map	Estimation from soil (<3 m depth) as well as geological and lithological (petrographic) maps (>3 m depth) Classification into 0 m, 3 m and 10 m
Soil parameters	Soil type/WRB classification system (2006/2007)	Reference Soil Group (List of RSGs)	1:25,000	Shapefile/WGS 84	Austrian soil map (ÖBK sheets 48, 49, 72, 79, 91, 108)	Translation from Austrian soil type to WRB classification system
Soil parameters	Soil texture/USDA classification system	Grain size distribution [mm] (weight percentage of sand, silt & clay)	1:25,000	Shapefile/WGS 84	Austrian soil map (ÖBK sheets 48, 49, 72, 79, 91, 108)	Transformation of the original data for an adequate application with regard to the three depth layers (reliable data only for the first depth layer)
Soil parameters	BD (Bulk Density)	g/cm ³	–	–	Self-generated classification set	This specific parameter is classified into three fixed classes, one for each possible depth layer: ■ layer 1 (0–3 m): 1.3 g/cm ³ ■ layer 2 (3–6 m): 1.5 g/cm ³ ■ layer 3 (6–10 m): 1.8 g/cm ³
Soil parameters	PSD (Pore Size Distribution)	Vol.-% (volumetric percentage values as a function of porosity equivalents in µm)	Respective values are explicitly assigned to each soil texture class	–	Self-generated classification set	This parameter is derived from soil texture data of the Austrian Soil Map (ÖBK) in combination with the bulk density and different soil moisture conditions
Administrative data, e.g. legal constraints, topographical maps, aerial photographs or satellite images	Legal constraints/protected areas	Occurrence: Yes/No	1:50,000	Shapefile/WGS 84	■ Salzburg Geographical Information System (SAGIS) from the Salzburg Federal Government ■ Geographical Information System of the Upper Austria Federal Government (DORIS)	Dataset comprises protection zones of lakes, landscape, mires, and nature protection areas

Table 3
Datasets used for the two German CSAs (case study areas).

Main parameter group	Parameter/Dataset description	Unit(s)	Scale/Resolution Accuracy of the dataset	File format/Projection	Data source(s)	Remarks and further information
Climate conditions	Annual and monthly average total precipitation	mm/month; mm/year	Resolution. 1 mm Scale: 1:25,000	Shapefile/WGS 84	German Meteorological Service (DWD)	For calculation of the Humidity Index
Climate conditions	Annual mean and minimum and monthly mean air temperature	°C	Resolution. 0.1 °C Scale: 1:25,000	Shapefile/WGS 84	German Meteorological Service (DWD)	For calculation of the Humidity Index and the volumetric heat capacity
Topographical and hydro-/geological parameters	Slope	° [degree]	Resolution: 1 m × 1 m	Shapefile/WGS 84	Bavarian Office for Land Surveying and Geoinformation (LVG)	Downscaled to 10 m × 10 m
Topographical and hydro-/geological parameters	Depth of the (ground) water table	Meters below surface [m]	1:50,000	Shapefile/WGS 84	Bavarian Environmental Agency (LfU): Hydrogeological maps of the test Areas (L 6330 Höchststadt, L 6530 Fürth)	For determination of saturated and unsaturated conditions within the soft rock zone (unconsolidated ground)
Topographical and hydro-/geological parameters	Depth of the soft rock zone/ Indication of the thickness	Metres below surface [m]	1:25,000	Shapefile/WGS 84	Bavarian Environmental Agency (LfU): Geological maps of the test areas (sheets GK 6431/6331; incl. information about the associated lithology)	Estimation based on interpretation of available geological, pedological and drill hole/ground investigation data
Soil parameters	Soil type/WRB classification system (2006/2007)	Reference Soil Group (List of RSGs)	1:25,000	Shapefile/WGS 84	Bavarian Environmental Agency (LfU): Concept soil maps of the test areas (sheets KBK 6431 Herzogenaaurach/KBK 6331 Röttenbach)	Transformation and application to the list of limitations
Soil parameters	Soil texture/USDA classification system	Grain size distribution [mm] (weight percentage of sand, silt & clay)	1:25,000	Shapefile/WGS 84	Bavarian Office for Land Surveying and Geoinformation (LVG): Soil maps according to the German fiscal soil estimation system (BSK 6431 Herzogenaaurach/6331 Röttenbach)	Additional use of drill hole/laboratory data and information from ground investigation in the Test Areas
Soil parameters	BD (Bulk Density)	g/cm ³	–	–	Self-generated classification set	This specific parameter is classified into three fixed classes, one for each possible depth layer: ■ layer 1 (0–3 m): 1.3 g/cm ³ ■ layer 2 (3–6 m): 1.5 g/cm ³ ■ layer 3 (6–10 m): 1.8 g/cm ³
Soil parameters Part B	PSD (Pore Size Distribution)	Vol.-% (volumetric percentage values as a function of porosity equivalents in µm)	Respective values are explicitly assigned to each exact soil texture class	–	Self-generated classification set	This parameter is derived from soil texture data in combination with the bulk density and different soil moisture conditions
Administrative data, e.g. legal constraints, topographical maps, aerial photographs or satellite images	Aerial photographs	–	Resolution: ■ 40 cm × 40 cm (Büchenbach) ■ 20 cm × 20 cm (Röttenbach)	GeoTIFF raster dataset	Bavarian Office for Land Surveying and Geoinformation (LVG): Digital aerial photographs of the test areas (DOP 40, DOP 20)	Additional data source for the geoscientific characterisation of the CSA

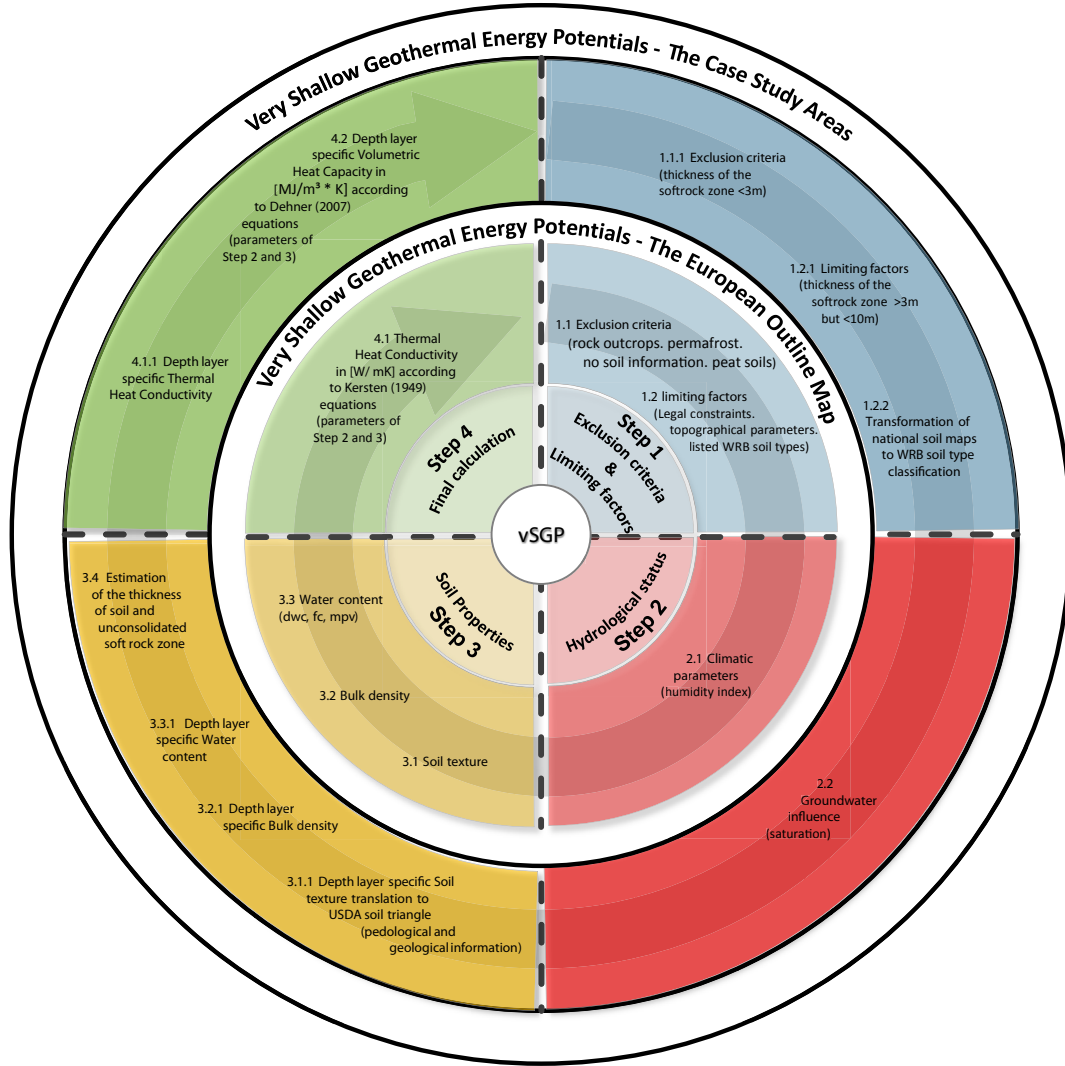


Fig. 2. The vSGP modelling approach for the CSAs (Case Study Areas).

protecting water resources, national or natural parks, Natura 2000 zones, and flood areas.

We consider the following soil types as unsuitable:

- Histosol (limited suitability due to very high share of organic material, e.g. peat),
- Cryosol (limited suitability due to impacts of frost and ice),
- Leptosol (limited suitability due to its extremely shallow and/or gravelly characteristic),

Table 4
Hierarchical levels regarding the assignment of pedological parameters to certain soil texture classes.

Quality level	Quality description
1	One of 12 classes in the USDA soil texture triangle can be allocated by the CSA information (e.g. from sieve analysis data or detailed maps)
2	Combination of two classes within the same group (one of four USDA soil texture groups)
3	One of the four main USDA soil texture groups can be allocated by the CSA information
4	Two of the four groups of the USDA soil texture triangle were merged

- Gleysol (limited suitability due to influence of groundwater), or
- Planosol (limited suitability due to impacts from abrupt textural discontinuities and stagnating water).

As national and CSA soil maps and respective soil types are considerably different, we used the WRB (World Reference Base) for Soils [46] with the respective RSGs (Reference Soil Groups) as a common denominator. Schema mappings from the national or CSA soil maps to the reference base have been applied.

The degree of slope also limits the installation of very shallow heat collector systems. Additional technical components for installation, venting and operating of these geothermal systems may be necessary. Country-specific digital elevation models with a 10–30 m resolution have been used to assign limitations at slopes greater than 15°.

2.5.3. Step 2: Hydrological status

Available climate stations within or close to the CSAs were used for the estimation of temperature and precipitation. With it we calculated the specific Humidity Index according to Schreiber [34]. However, since the soil water content plays an important role in the heat transport within the soil [43], areas with saturated soil conditions have been further investigated.

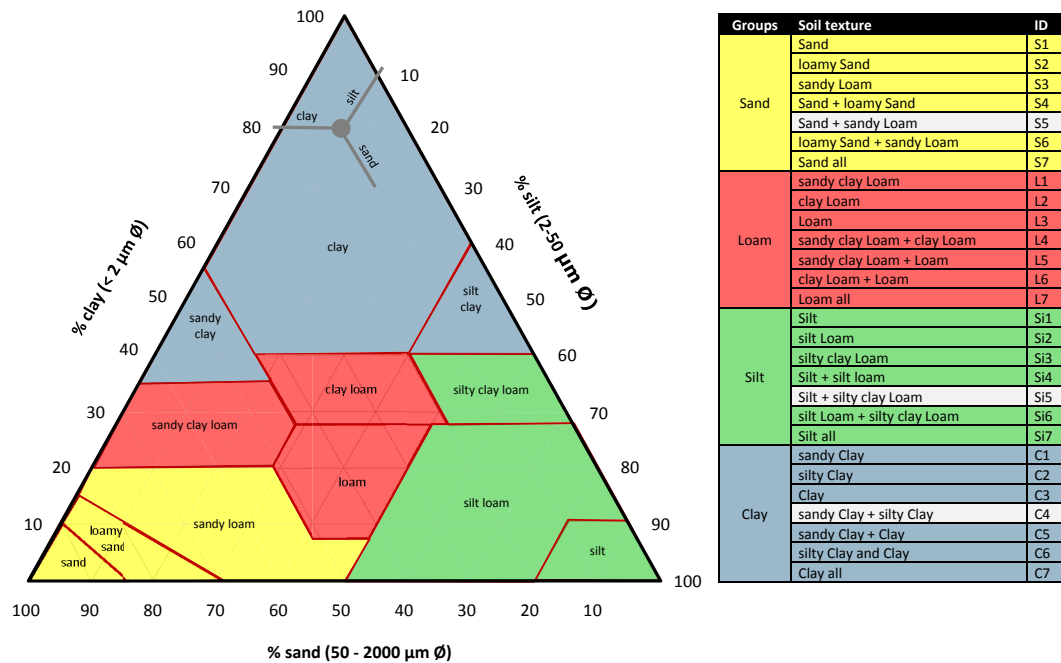


Fig. 3. Texture classes according to the USDA texture triangle grouped to 12 single classes or four aggregated groups.

Each soil texture class shows a characteristic PSD (pore size distribution). Obtaining this information requires soil texture information with hydrological data regarding the depth of the water table to describe the prevailing geothermal conditions. In sandy soils with a high ac (air capacity), the TC is reduced because air is a good heat isolator. In case of saturated conditions, the entire pore system of the soil matrix is filled with water (sum of ac + fc (field capacity)). With increasing water content, the conditions for

conductivity of heat in the soils generally increase and thus show the highest values. We combined soil texture data with hydrological data for using related formulae to estimate the vSGP (very shallow geothermal potential).

Water saturation of one or more depth layers can occur through groundwater influence. The information about saturation was derived from hydro(geo)logical datasets, or from the description of borehole data and wells. In case of complete soil water saturation we considered the ac combined with the fc, which allows a feasible statement about the total pore volume in case of full water saturation.

2.5.4. Step 3: Soil properties

While Bertermann et al. [14] could not distinguish between different depth layers in the EOM, the national soil maps, the geological maps and/or drilling information provided soil texture information in different depths. The grain size distribution of the soil matrix (0–3 m) and subjacent ground matrix (3–10 m) is considered the key factor for the calculation of the TC and the VHC according to the methodology and equations developed by Kersten [47] and Dehner [48].

The accuracy level of the determined soil texture varies amongst the CSA datasets. Thus it was necessary to indicate the quality of the soil texture information (see Table 4).

Depending on the soil texture data quality in the CSAs, we used different soil texture classes according to the USDA (United States Department for Agriculture) soil texture triangle [49]. Quality level 1 from Table 4 corresponds with the 12 main classes in Fig. 3, while quality level 3 corresponds with the four coloured groups Sand (yellow), Loam (red), Silt (green) and Clay (blue) as a merge of three similar classes with regard to the pedo-physical characteristics for each group. The quality levels 2 and 4 consider a specific combination of classes or groups from the USDA soil texture triangle. These combinations are explained below.

Dependent on the national classification system of soil texture, the grain size distribution was harmonised according to the USDA soil texture triangle. The transformation to the USDA soil texture

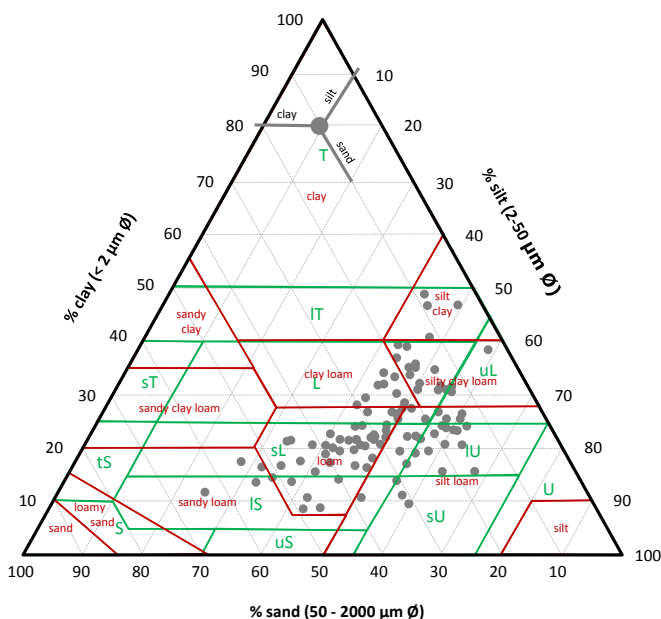


Fig. 4. Example of the Austrian L1050 soil texture triangle (green) overlapping the USDA triangle (red) with soil texture data from the Mondsee catchment (grey). (For interpretation of the references to colour in this figure legend, the reader is referred to the web version of this article.)

Table 5
PSDs (pore size distributions) of soil texture quality class 1 depending on the assigned BD (bulk density) values.

Soil texture-classes according to the USDA classification	Air capacity (ac) Porosities > 50 μm (pF < 1.8)			Field capacity (fc) Porosities \leq 50 μm (pF \geq 1.8)			Dead water content (dwc) Porosities \leq 0.2 μm (pF \geq 4.2)		
	0-3	3-6	6-10	0-3	3-6	6-10	0-3	3-6	6-10
Depth layer [m]	0-3	3-6	6-10	0-3	3-6	6-10	0-3	3-6	6-10
Bulk density [$\frac{g}{\text{cm}^3}$]	1.3	1.5	1.8	1.3	1.5	1.8	1.3	1.5	1.8
Sand	36	32	27	14	11	10	5	4	3
loamy Sand	24	21	15	26	23	20	7	6	5
sandy Loam	18	14	10	34	29	26	11	9	8
sandy clay Loam	15	12	7	39	31	28	21	16	16
clay Loam	10	6	4	44	37	33	26	24	22
Loam	14	9	6	39	33	30	17	16	15
Lilt	10	7	3	43	38	35	13	12	12
silt Loam	11	7	4	40	36	34	16	14	14
silty clay Lloam	8	6	3	45	38	35	28	25	25
sandy Clay	7	6	5	45	37	32	29	24	21
silty Clay	5	4	3	47	42	36	31	30	26
Clay	5	4	3	49	41	35	33	28	23

triangle was done by either class–class mapping, or mapping of the weight percentages of sand, silt and clay (Fig. 4). This procedure applies to all three depth layers where information is available.

The USDA soil texture classes and information on BD is used to estimate the parameters ac, fc and dwc (dead water content). The BD classes reflect unconsolidated soils becoming more compacted with increasing depth, and thus for instance decrease the ac. Since for most CSAs detailed spatially explicit BD information was not available, we assigned the following BD values to the three depth layers:

- from 0 to 3 m \rightarrow 1.3 g/cm³
- from 3 to 6 m \rightarrow 1.5 g/cm³
- from 6 to 10 m \rightarrow 1.8 g/cm³

For each soil texture quality class and each BD class we assigned volume percentage values for the parameters ac, fc and dwc (Tables 5–7) after Ad-hoc-AG-Boden [50] and Kuntze et al. [51].

According to Table 4, combinations of different soil texture classes are possible in quality levels 2 and 4. Combinations of two

Table 6
PSDs (pore size distributions) of the soil texture quality class 3 depending on the different BD (bulk density) values.

Main soil texture groups according to the USDA classification	ID	Air capacity (ac) Porosities > 50 μm (pF < 1.8)			Field capacity (fc) Porosities \leq 50 μm (pF \geq 1.8)			Dead water content (dwc) Porosities \leq 0.2 μm (pF \geq 4.2)		
		0-3	3-6	6-10	0-3	3-6	6-10	0-3	3-6	6-10
Depth layer [m]		0-3	3-6	6-10	0-3	3-6	6-10	0-3	3-6	6-10
Bulk density [$\frac{g}{\text{cm}^3}$]		1.3	1.5	1.8	1.3	1.5	1.8	1.3	1.5	1.8
Sand	S7	26	22	17	25	21	19	8	6	5
Loam	L7	13	9	6	41	34	30	21	19	18
Silt	Si7	10	7	3	43	37	35	19	17	17
Clay	C7	6	5	4	47	40	34	31	27	23

Table 7
Soil properties based on the combinations of quality class 2 depending on the different BD (bulk density) values.

Combination of the soil texture classes according to the USDA classification	ID	Air capacity (ac) Porosities > 50 μm (pF < 1.8)			Field capacity (fc) Porosities ≤ 50 μm (pF ≥ 1.8)			Dead water content (dwc) Porosities ≤ 0.2 μm (pF ≥ 4.2)		
		0-3	3-6	6-10	0-3	3-6	6-10	0-3	3-6	6-10
Depth layer [m]										
Bulk density [$\frac{g}{cm^3}$]		1.3	1.5	1.8	1.3	1.5	1.8	1.3	1.5	1.8
Sand + loamy Sand	S4	30	27	21	20	17	15	6	5	4
Sand + sandy Loam	S5	27	23	19	24	20	18	8	7	6
loamy Sand + sandy Loam	S6	21	18	13	30	26	23	9	8	7
sandy clay Loam + clay Loam	L4	13	9	6	42	34	31	24	20	19
sandy clay Loam + Loam	L5	15	11	7	39	32	29	19	16	16
clay Loam + Loam	L6	12	8	5	42	35	32	22	20	19
Silt + silt Loam	Si4	11	7	4	42	37	35	15	13	13
Silt + silty clay Loam	Si5	9	7	3	44	38	35	21	19	19
Silt loam + silty clay Loam	Si6	10	7	4	43	37	35	22	20	20
sandy Clay + silty Clay	C4	6	5	4	46	40	34	30	27	24
sandy Clay + Clay	C5	6	5	4	47	39	34	31	26	22
silty Clay + Clay	C6	5	4	3	48	42	36	32	29	25

similar soil texture classes cause changes to the values of ac, fc and the dwc. For simplicity reasons we applied Equation (1) to interpolate between soil texture classes and the PSD values.

Calculation of soil properties based on soil texture class combinations

$$c = \left(\frac{a + b}{2} \right) \quad (1)$$

Considering that other averaging methods might yield slightly deviating results, the approximation in Equation (1) is considered to sufficiently provide exact values as shown in Table 7. Gray-coloured combinations “silty Clay + sandy Clay”, “silty clay Loam + Silt”, as well as “Sand + sandy Loam” are not practice-relevant because the individual soil texture classes are not neighbouring. This does not allow a useful average determination of the individual PSDs for further calculations.

2.5.5. Step 4: Final calculation

Based on the PSD values (step 3), the assigned BD values for different depth layers, and the determined soil texture class, the TC and VHC were calculated according to the equations provided by Kersten [47] and Dehner [48].

2.5.5.1. TC, λ . The TC is expressed by λ . Dependent on the quality of the national soil texture classes and the allocation done in step 3, either the 12 soil texture classes (Fig. 5, A), or the 4 soil texture groups (Fig. 5, B) are considered for the separation of sand shares smaller or greater than 50%. For the combined soil texture classes according to Table 4 (e.g. quality level 2), the classes C5, L4, L5 indicated in Fig. 3 form a special case. Despite varying shares of sand across the class combinations, they will be assigned to the class >50% since the sand component positively influences the TC due to a higher share of high conductive quartz [52]. Dependent on these before mentioned separations, Equation (2) or (3) applies.

For sand percentages >50%

$$\lambda = 0.1442 * \left(0.7 * \left(\lg \frac{\text{PSD}}{\text{BD}} \right) + 0.4 \right) * 10^{(0.6243 * \text{BD})} \quad (2)$$

For sand percentages <50%

$$\lambda = 0.1442 * \left(0.9 * \left(\lg \frac{\text{PSD}}{\text{BD}} \right) - 0.2 \right) * 10^{(0.6243 * \text{BD})} \quad (3)$$

Units	
Thermal Conductivity	$\lambda = \frac{W}{m^2K}$
Water content	$w = [\text{percent by weight}]$
Pore Size Distribution	$\text{PSD} = [\text{Vol.-%}]$
Bulk Density	$\text{BD} = \left[\frac{g}{cm^3} \right]$

2.5.5.2. VHC, Cv. Finally the PSDs as calculated in step 3 are used to calculate the VHC (Equations (4)–(6)).

Specific quantity of heat of dry rock (Cs) as a function of temperature

$$C_s = 1.64 * T + 704 \quad (4)$$

Specific heat capacity per mass unit (Cp) as a function of water content (w)

$$C_p = \frac{100 * C_s + 4190 * w}{100 + w} \quad (5)$$

With the water content as a function of PSD (pore size distribution) and BD

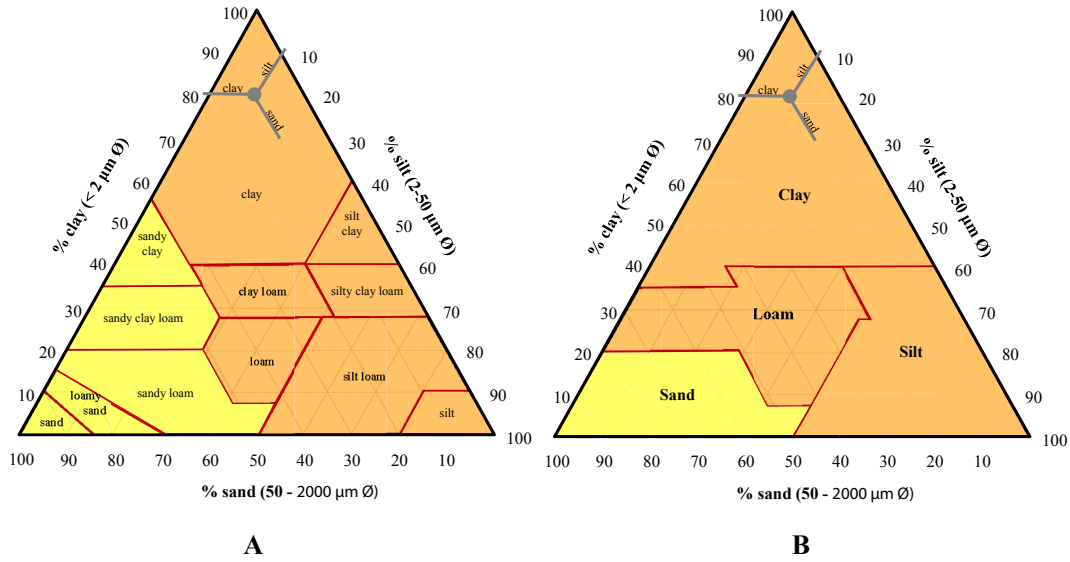


Fig. 5. The modified USDA soil texture classifications showing shares >50% sand (yellow) and <50% (orange) for A) the twelve classes (quality level 1 & 2) and B) the aggregated four groups (quality level 3 & 4). (For interpretation of the references to colour in this figure legend, the reader is referred to the web version of this article.)

$$w = \frac{PSD}{BD}$$

VHC per mass unit (Cv) as a function of water content (w) and BD

$$Cv = BD * Cp \tag{6}$$

Only at this explicit step of calculation, the unit of the BD has to be specified

$$BD = \frac{kg}{m^3}$$

Units	
Soil temperature to be derived from air temperature data	$T = [^{\circ}C]$
Specific quantity of heat	$Cs = \frac{J}{kg^{\circ}K}$
Specific heat capacity	$Cp = \frac{J}{kg^{\circ}K}$
Volumetric Heat Capacity	$Cv = \frac{J}{m^3^{\circ}K}$
Water content	w = percent by weight
Pore Size Distribution	PSD = [Vol.-%]
Bulk Density	$BD = \left[\frac{g}{cm^3} \right]$ for calculation of Cv :
	$X \left[\frac{g}{cm^3} \right] = X \left[\frac{kg}{dm^3} \right] = X * 1000 \left[\frac{kg}{m^3} \right]$

2.6. Validation procedures

For validation of the soil properties exposed in the soil maps and the calculated TC values, soil samples were taken from the CSAs. In the laboratory the water content and the BD were evaluated according to standard procedures [53,54], while the soil texture was analysed with SediGraph [55]. Afterwards, TC was measured with the TK04 measuring instrument [56]. The half-space probes were used to get the absolute TC values. The surface of solids was ground and smoothed and a moderate contact pressure between 5 and 10 bar was applied to ensure good contact between the probe and the sample surface. Due to the artificial pressure applied when

using the TK04 instrument, the BD of the probes increased. To be able to compare the laboratory TC values with the modelled ones, a count back of TC values to the pre-defined bulk densities (depending on the depth layer the sample is taken from) is required. This was done under the premises of a direct linear relationship between TC and BD.

2.7. The visualisation system

While Bertermann et al. [14] used data storage facilities at the central server only, the information sources of the 14 CSAs from the nine countries are spread across different CSA servers. Thus, the spatial datasets used (e.g. Tables 2 and 3) remain on the individual CSA server. Upon a client map request via a web browser, the central server receives a WMS (Web Map Service, [57]) response from the CSA server. Based on the same structure of the pre-processed input datasets and the final results, the compliance to OGC standards (Open Geospatial Consortium) with for instance the SLD (Styled Layer Descriptor, [58]) ensures the retrieval of user requested information from the client system in a unified legend. This is independent of the map server technologies used at the CSA servers (e.g. ESRI ArcGIS Server, open-source GeoServer) (Fig. 6).

3. Results

3.1. Main results

As a result the TC is illustrated as the main parameter within the publicly available TMMV (<http://thermomap.mapviewer.sbg.ac.at/>). For each CSA the TC calculated in step 4 is displayed in five classes in up to three different map layers depending on the locally available depth. The graduated map of these five classes shows low (blue) to high (red) vSGP, whereby blank colour refers to excluded areas where no information is available (Fig. 7). The hatchings in the two deeper map layers indicate areas where the depth is not completely available for installations due to soft rock limitations; whilst the additional blue hatched map layer indicates usage limitations like protection zones, unsuitable soil types or slope >15°.

The results and a range of supportive background parameters used in steps 1–4 can be queried with the “vSGP Infobox” tool

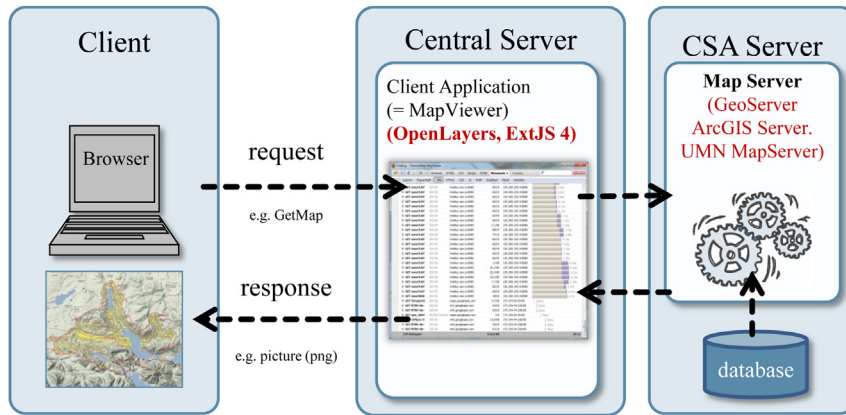


Fig. 6. The WebGIS architecture.

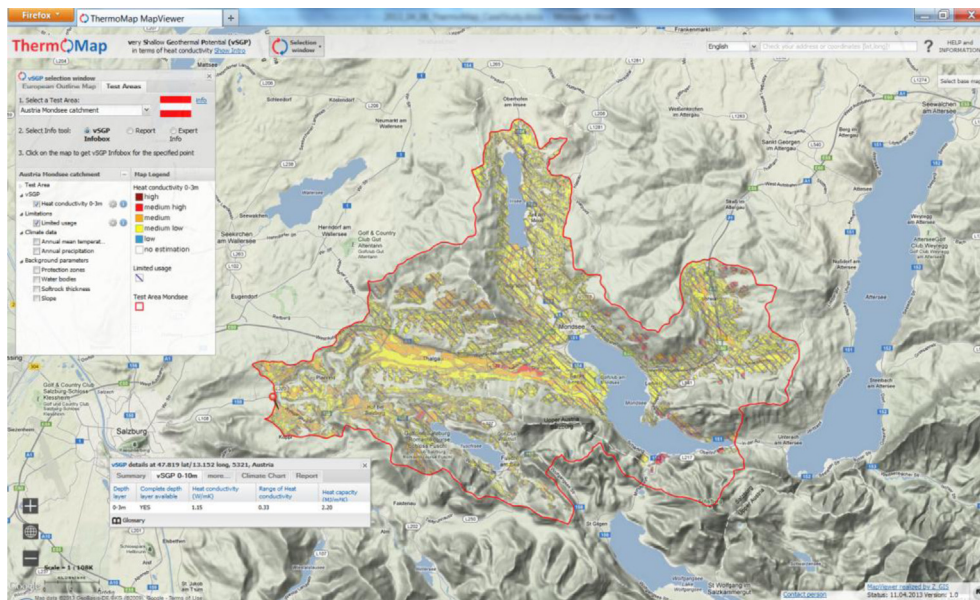


Fig. 7. The CSA Mondsee visualising the vSGPs (very shallow geothermal potentials) in the TMMV (ThermoMap MapViewer).

compiled for all available depth layers. It contains e.g. data about the parameters soil texture, BD, PSD, precipitation (average month/year), air temperature (average month/year), and thickness of the soft rock zone and the VHC value.

The two German and the Austrian CSA TC values vary between 1.6 W/m²*K and 2.2 W/m²*K for the first depth layer. Here the highest average, and thus the highest potential for vSGP exploitation, is found in the CSA Büchenbach. As indicated in Table 8 the values also vary between the different depth layers. However, the CSA Röttenbach indicates higher potentials in the second depth layer.

The areas excluded in Table 8 are water bodies and areas with a soft rock thickness of <3 m or less than the respective depth layer. The limited areas consist of protection zones, unsuitable soil types and a slope of >15°, but also of not completely available depth layers (only second and third depth layer affected). Since e.g. the soft rock thickness in the CSA Büchenbach does not go beyond 5.7 m depth, the complete second depth layer (3–6 m) is to 100% assigned as limited area.

The VHC values are not displayed spatially explicit, but can be retrieved from the vSGP Infobox as shown in Fig. 7. Additional information about the spatial distribution can be requested by the

Table 8
The min, max, and average TC values per CSA and depth layer.

Case study area	Depth layer [M]	Min λ [W/m ² *K]	Max λ [W/m ² *K]	Mean λ [W/m ² *K]	Excluded area [% of the CSA]	Limited area [% of the potential area]
Mondsee	0–3	1.06	1.30	1.09	16.57	59.86
Büchenbach	0–3	1.17	1.43	1.37	1.60	19.52
	3–6	1.41	1.77	1.64	79.77	100.00
Röttenbach	0–3	1.22	1.34	1.29	0.00	0.00
	3–6	1.62	1.78	1.67	0.00	65.81
	6–10	2.50	2.51	2.51	65.78	100.00

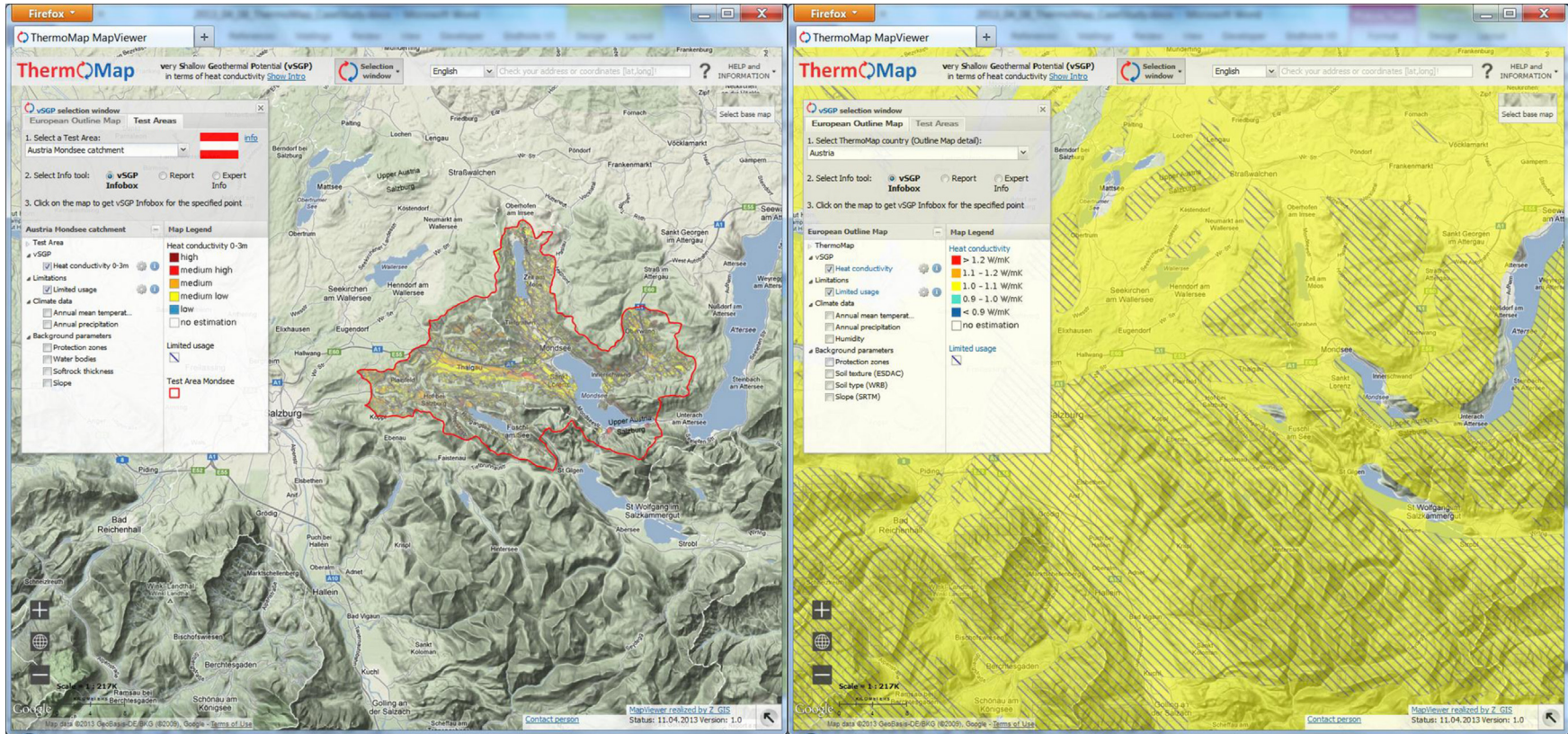


Fig. 9. Comparison of the CSA Mondsee with the respective area of the EOM.

user either checking the layers on limitation areas or different background parameters. Another option is to switch to the TMMV expert mode. Here a table of all calculated values of the respective visible depth layer for a specified point in the CSA can be obtained. Similar to Table 9, all possible TC values (λ) are listed for the respective depth layer as a result from the equations explained in step four. The values of Table 9 can be read off for each soil texture class or category of combination, as well as for each soil water condition (dwc, fc, ac).

3.2. Different system conditions

In general, 11 different system conditions can be observed in the CSAs (Fig. 8, I–XI). The respective system status results from the saturated and unsaturated depth layers (see Step 2). All possible hydrological system statuses and different depth layers are shown in Fig. 8, where the cases I–IV describe unsaturated conditions and

the cases V–XI reflect saturated conditions with groundwater influence.

System status (I) characterises only hard rock with missing or sparse vegetation. These areas are considered as excluded since instalments will not take place here with present technologies. System status (II) describes the first depth layer (0–3 m), as well as the first BD class for unsaturated conditions. System status (III) describes the first two depth layers (0–6 m), as well as the first and second BD class for unsaturated conditions. System status (IV) describes all three depth layers (0–10 m) and all three BD classes for unsaturated conditions. System status (V) is the first one influenced by groundwater. All three depth layers are influenced by groundwater, so that not only minimum (dwc) and maximum (fc) values of PSD, but also the values for the saturated layers (fc + ac) have to be used. System status (VI) shows the first depth layer as unsaturated. For the following two layers, saturated conditions are valid. System status (VII) describes the first two depth layers as unsaturated. The

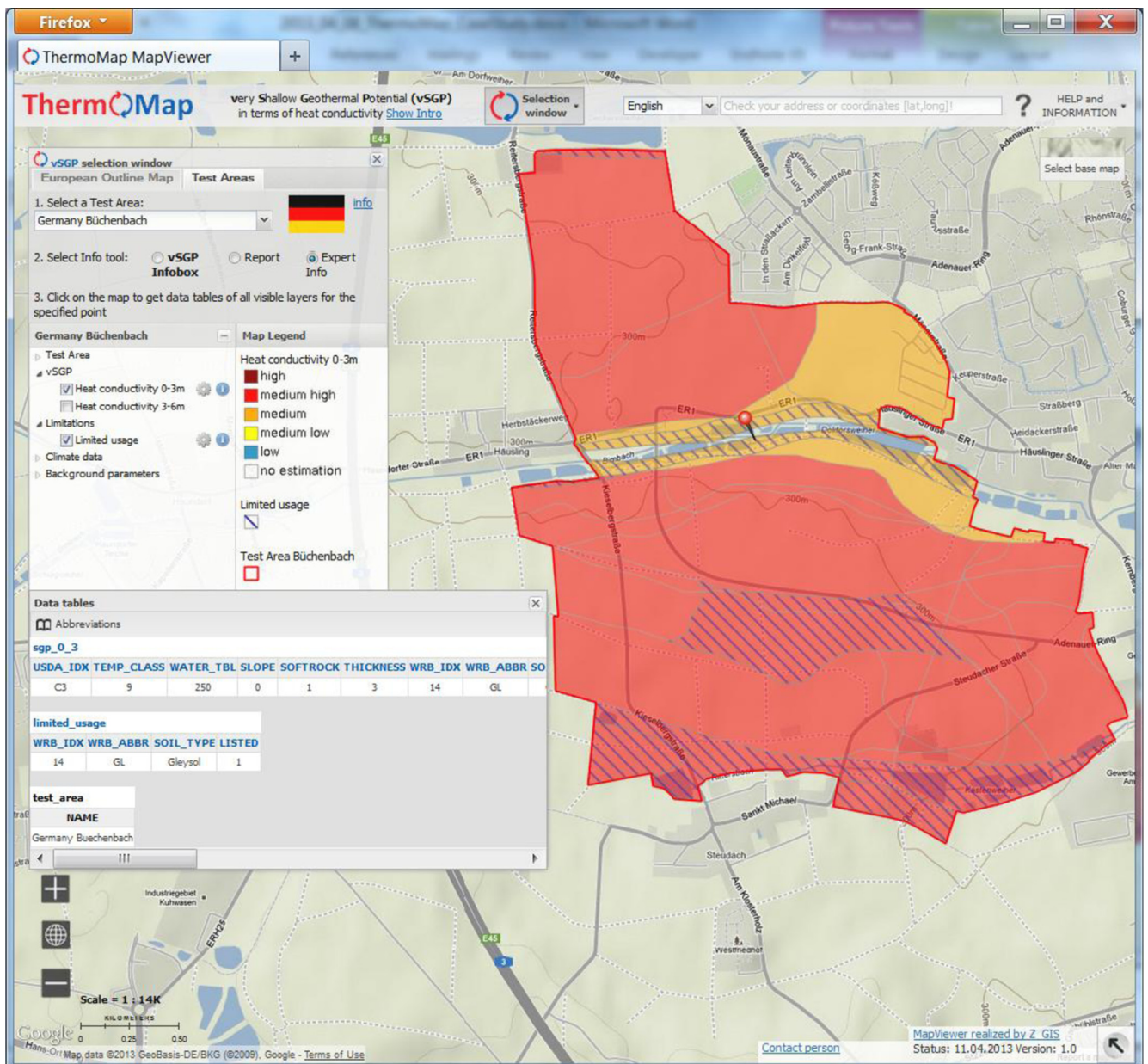


Fig. 10. The German CSA Büchenbach.

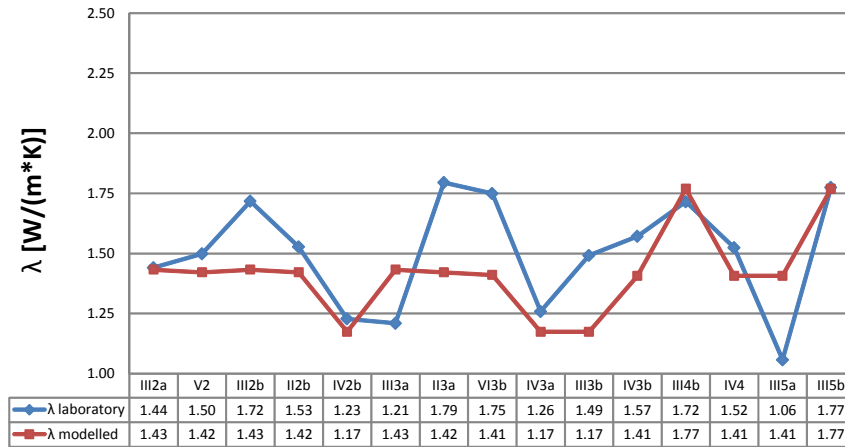


Fig. 11. Comparison of laboratory investigation and modelled TC (thermal conductivity) values at saturated conditions in the German CSA Büchenbach.

third depth layer (deep depth layer) is under saturated conditions. In system status (VIII) only the first two depth layers are available. Both are saturated. In system status (IX) only the first two depth layers are available. The second depth layer is saturated. In system status (X) only the first depth layer is available under saturated conditions. As with system status (I), system status (XI) contains consolidated rock with missing or sparse vegetation which is saturated with water. Additional statuses are possible in case of only partly available depth layers. The system conditions can be reviewed in the report function of the TMMV vSGP Infobox for each of the CSA where the TC has been calculated.

3.3. The Austrian case study at landscape scale

The vSGP modelling results as presented in Fig. 7 and Table 8 show large areas with no information. These are excluded areas where rock crops out, the thickness of the soft rock zone is <3 m, or which are dominated by forests. Hatchings inform about huge areas which are usable under limited conditions. Very wet soils (Gleysols) and Planosols dominate the restrictions, but also the maximum availability of only 3 m depth limits the exploitation potential at greater depths. However, the central Fuschler Ache Valley east to the lake Mondsee exposes the highest exploitation values. Also of high suitability are the higher populated areas Koppl and Hof which are of main interest due to new settlement expansion places.

To demonstrate the downscaling advancements of this approach, we compared the CSA Mondsee with the respective area of the EOM developed by Bertermann et al. [14] (Fig. 9). The areas assigned with limitation or exclusion criteria are well represented in both maps. The TC values in the CSA Mondsee vary in space and depth, but altogether range from medium low 1.06 W/m²K (yellow) over medium 1.15 W/m²K (orange) to medium high with 1.3 W/m²K (light red). The respective value obtained from the EOM is 1.07 W/m²K (yellow). Thus, in this case the EOM underestimates the local vSGP.

3.4. The German case studies at local/site scale

The results in Büchenbach at a local scale are assigned as having limited potential due to the presence of Planosols and Gleysols (19.5% in the first depth layer). Limited zones of unconsolidated soils occur in the deeper depth layer (Fig. 10).

Comparisons of the modelling results with the laboratory measurements are shown in Fig. 11 and Table 10 for Büchenbach, and Fig. 12 and Table 11 for Röttenbach.

Measurement results of the TK04 (half-space probe) were based on relatively high BD values due to the mentioned compression needed for the measurement process. This required an adaptation to the pre-defined BD classes depending on the respective depth layer mentioned above. Under the premise of a linear relationship

Table 10

Sample depth and corresponding depth layer from the CSA Büchenbach.

Sample ID	Depth [m]	Depth layer	Difference interpolated vs. modelled [W/(m ² K)]	Difference interpolated vs. modelled [%]
III2a	1.0–1.3	1	0.01	0.58
V2	1.0–2.0	1	0.08	5.38
III2b	1.3–1.8	1	0.29	19.89
II2b	1.5–2.0	1	0.11	7.44
IV2b	1.5–2.1	1	0.06	4.56
III3a	1.8–2.3	1	−0.22	15.56
II3a	2.0–2.7	1	0.37	26.24
VI3b	2.05–2.3	1	0.34	24.02
IV3a	2.1–3.0	1	0.09	7–20
III3b	2.3–2.8	1	0.32	27.02
IV3b	3.0–3.6	2	0.16	11.67
III4b	3.2–3.8	2	−0.05	3.05
IV4	3.6–4.0	2	0.11	8.29
III5a	3.8–4.1	2	−0.35	24.79
III5b	4.1–4.8	2	0.00	0.31

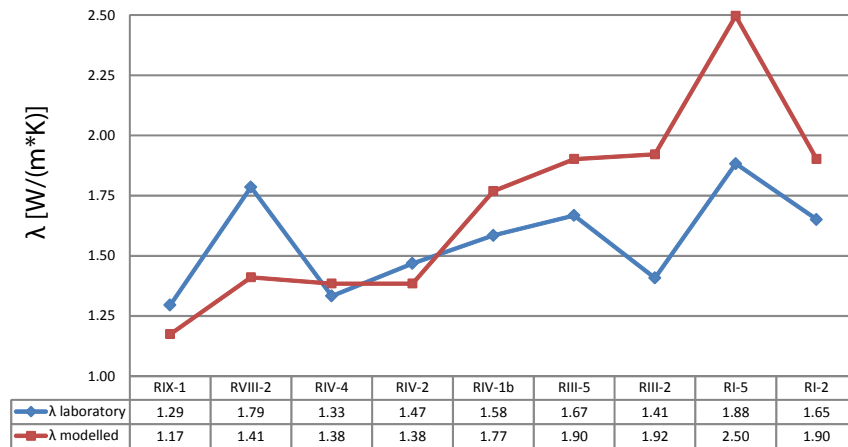


Fig. 12. Comparison of laboratory investigation and modelled thermal conductivity values at saturated conditions in the German CSA Röttenbach.

function of TC and BD, the results show that in many cases the modelling result underestimates the real values, while in a few cases the estimations are almost identical.

The graphs in Figs. 11 and 12 show the TC values according to the different sample depth, respectively presented in Tables 10 and 11. While the CSA Büchenbach does not show a significant increase in TC values with increasing soil depth, the CSA Röttenbach shows a trend of proportionally increasing TC with soil depth. For both test areas the deviation between modelled values and laboratory findings range from 79% (underestimation) to 136% (overestimation). As an average deviation, Büchenbach slightly underestimated the laboratory findings by about 4% with a standard deviation of 15%, while the CSA Röttenbach overestimated the laboratory finding by about 9% with a standard deviation of 19%.

A comparison of the first depth layer (0–3 m) of the CSA Büchenbach with the respective area in the EOM results in similar findings as for the Mondsee CSA. The values in the CSA Büchenbach range from 1.1 to 1.4 W/m²K compared to 1.2 W/m²K in the EOM. The same is valid for Röttenbach with values ranging from 1.2 to 1.6 W/m²K in the CSA and 1.2 W/m²K in the EOM.

On a site specific scale, the spatial differences of the TC in the CSA Röttenbach are less apparent as for instance in the CSA Büchenbach or the CSA Mondsee. TC values in Röttenbach range from 1.2 to 1.6 W/m²K. Only two class values with no limitations are available in the first depth layer (Fig. 13).

4. Discussion and conclusion

When considering that huge proportions of energy are used for heating and cooling purposes [59], it becomes evident that the thermal capacities of the ground can contribute to energy savings

and CO₂ reductions [60]. The fact that there are almost no legal restrictions, makes the exploitation of the very shallow geothermal energy even more attractive [61].

We demonstrated that downscaling the vSGPs from the European to landscape, or even local scale is possible with the advanced methodology presented. Each of the 14 CSAs visualised in the TMMV proved successful in acquiring and processing the required datasets. Harmonisation towards a unified and comparable result was both technically and methodologically feasible. Nevertheless, we faced some challenges and opportunities. The existing datasets used here come in heterogeneous file formats and there is a specific set of attributes for each dataset. These attributes represent a data provider's internal data model. Standardised transformation schemas – as intended by the presently on-going INSPIRE process – aim for the interoperability of these datasets in defining a common data schema [62]. Since these data schemata for different environmental datasets have not yet been completed, we defined the approach outlined here; but once these schema transformations towards a common data model are finished, this would allow the exchange, combination, comparison and integration of different datasets from different distributed sources.

The most important parameters are soil texture, determined for the three depth layers, and BD. The soil texture determines the PSD according to the BD class, whereas the mean annual temperature and precipitation given by the local climatic conditions provide the hydrological soil conditions. Using the mentioned formulae for the Humidity Index, a specific pedological water and air status within the soil and soft rock zone can be assumed for sub-/arid conditions (dwc status), sub-/to per-/humid conditions (fc status) or saturated conditions due to groundwater influence (mpv status = fc + ac). Thus, appropriate exact values can be applied for each hydrological

Table 11
Sample depth and corresponding depth layer from the CSA Röttenbach.

Sample ID	Depth [m]	Depth layer	Difference interpolated vs. modelled [W/(m ² K)]	Difference interpolated vs. modelled [%]
RIX-1	0.00–1.00	1	0.12	10.27
RVIII-2	1.42–1.80	1	0.38	26.58
RIV-4	5.05–5.25	2	−0.05	3.75
RIV-2	5.35–5.55	2	0.09	6.01
RIV-1b	5.55–5.65	2	−0.19	10.43
RIII-5	6.55–6.70	3	−0.23	12.33
RIII-2	7.25–7.35	3	−0.51	26.73
RI-5	9.50–9.60	3	−0.62	24.58
RI-2	9.95–10.00	3	−0.25	13.20

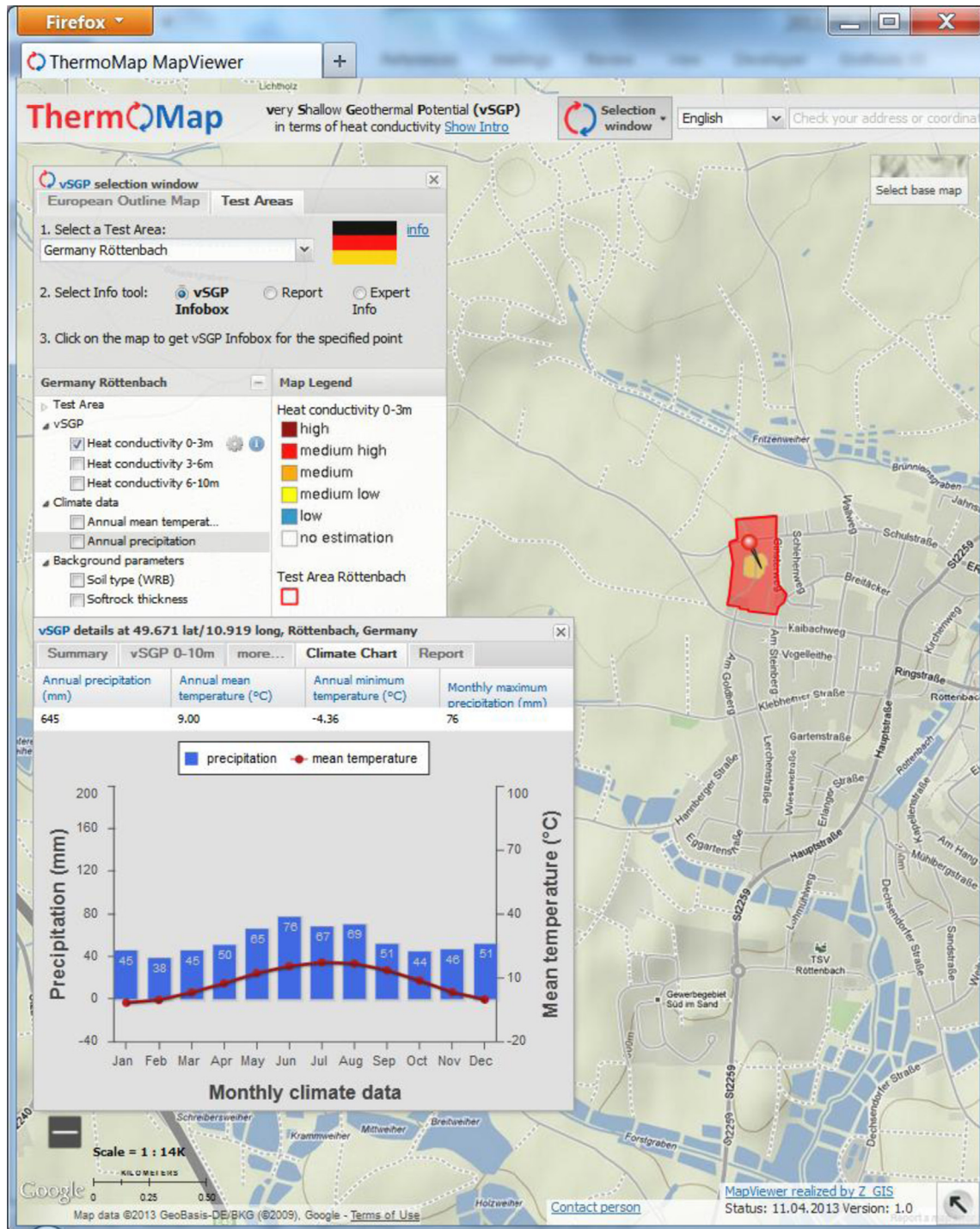


Fig. 13. The German CSA Röttenbach highlighting climate information in the vSGP Infobox.

status. The technical and semantical schema mapping for the conversion of soil texture information from national and local datasets to the USDA soil texture triangle is crucial for the estimation of TC. This result is similar to the findings outlined by Klug and Bretz [63] on behalf of the GS Soil consortium.

The comparison between the EOM and the first depth layers of the CSA maps generally show slightly differing results. These differences result from the underlying datasets and its attribute quality and spatial accuracy. We could identify that the EOM slightly underestimates the values we modelled at CSA level, since

the EOM does not take into account saturation information. This results from higher quality data used in the CSA and the possibility to differentiate between three depth layers.

Not only does the TC vary with depth, but also the spatial pattern of the TC values in the CSA approach is equally diverse. Thus, especially for smaller planning districts like the CSA Röttenbach, the CSA information is of higher value to geothermal implementation companies than the EOM information.

As shown in Figs. 11 and 12, laboratory measurements might obtain slightly different values, thus, the spatial TC pattern might

be even more diverse than shown in the CSA maps. This is due to the local invariances which have been aggregated in the utilised datasets (e.g. soil or geological maps). Furthermore, special (micro-) climatological and hydrological site conditions, herein not accounted for, have an impact on the real in situ TC. In general, the TC values modelled here – as compared to the laboratory findings – are similar to the differences of $\pm 25\%$ as mentioned in Kersten [47]. These uncertainties from real potentials and the CSA modelling might result from applied pedotransfer functions in general [64,65], or more specifically discrepancies between the PSD and the water retention curve of a soil type [66]. Differences from laboratory and modelled vSGP values might also result from other causes, e.g. the choice of analytical methods used and the pre-sample treatment often has consequences, for instance for the shape of particle-size distribution [67]. These then in turn affect the evaluation of soil textural parameters. Carrick et al. [68] also show the unsuitability of small field probes “for measuring water-movement attributes, due to their potential to provide unrealistic representation of macro-pore connectivity and abundance hydraulic characterization”.

Comparisons of the CSAs with the EOM always result in a slight underestimation of TC values in the EOM. Thus, with increasing scales from 1:250,000 to 1:50,000/1:5000, we received higher TC values. These values withstand the laboratory findings as tested in the German CSAs. As we used a standardised modelling approach, and the laboratory findings correspond with the modelling results in the two tested areas, we assume the transfer to other CSAs proved successful and thus TC comparisons across CSAs are valid.

The time scale of analysis is based on annual average values. Thus, occurring seasonal changes of, for instance, BD and the saturation conditions as described by Hu et al. [69], or the effect of different air pressures on the TC [70] remain unattended. Furthermore, variations in different farming systems as for instance tilled soils [71] also remain unattended since after installation of a very shallow geothermal system, the specific pedological structure will be changed anyway. Additionally, we did not take into account ground heat storage possibilities from solar collectors as for instance analysed by Kroll and Ziegler [72]. Thus much higher vSGP might be available locally when combining different RES exploitations.

We conclude that the methods developed for estimating the vSGP based on existing and available digital datasets can be applied to both the pan-European and the case study level. The general characteristics at both levels demonstrate the capability of the proposed procedure for locating sources of low to high vSGP. The procedures developed here are found to be a robust (withstand laboratory measurements), fast (retrieval of maps in the TMMV), effective (the possibility to use existing sources for modelling the value of vSGP) and efficient (measure of success in increasing the information level before and after the modelling) method for detecting vSGP.

Finally it is important to acknowledge the different scales used in the EOM and the CSA approach described here. While the pan-European approach (covering the whole of Europe) has been designed to inform European politics about the vSGP in a broad manner, the CSA approach provides information only in 14 selected test areas. However, the CSA approach has been designed for environmental or residential planning guidelines to be used by governments, but also single public users who are interested in alternative energy resources for cooling and heating their residential or business buildings.

5. Outlook

Since information on the vSGP at a landscape to local scale is only available in 14 CSAs, huge parts of Europe presently have not

been analysed regarding their vSGP. However, the INSPIRE Directive foresees comprehensive data schemata for 34 data themes as listed in the three Annexes of the directive. At the same time, responsible national agencies need to provide schema mapping procedures from their datasets complying with the INSPIRE schema. We recommend continuing the schema mappings works to ensure a seamless view on environmental datasets and their attributes. Progress should be made in finding all these technically and semantically harmonised datasets, which can then find their way into this modelling approach and would provide a pan-European picture of vSGPs based on high-resolution national datasets.

Acknowledgements

This research has been co-financed by the EC ICT PSP project “ThermoMap” (250446). We would like to take this opportunity to thank for the good and constructive working relationship among the ThermoMap consortium. We are also thankful to Reinhold Roßner for his helpful review and useful comments on earlier versions of this article. Unfortunately he died quite early in the developments of this article. In addition we would like to thank all consortium partners, especially Mario Psyk (Rehau AG + CO) who provided us with helpful comments from the business domain and Christopher Weindl for providing the laboratory data from the German CSAs (Case Study Areas). We also would like to acknowledge the Doctoral College GIScience (DK W 1237-N23) of the University of Salzburg providing continuous support based on funding received from the Austrian National Science Fund (FWF).

References

- [1] Sims REH. Renewable energy: a response to climate change. *Sol Energy* 2004;76(1–3):9–17.
- [2] Duić N, Guzović Z, Lund H. Sustainable development of energy, water and environment systems. *Energy* 2011;36(4):1839–41.
- [3] Eicker U, Vorschulze C. Potential of geothermal heat exchangers for office building climatisation. *Renew Energy* 2009;34(4):1126–33.
- [4] Breesch H, Bossaer A, Janssens A. Passive cooling in a low-energy office building. *Sol Energy* 2005;79(6):682–96.
- [5] Jacovides CP, Mihalakakou G, Santamouris M, Lewis JO. On the ground temperature profile for passive cooling applications in buildings. *Sol Energy* 1996;57(3):167–75.
- [6] Costa VAF. Thermodynamic analysis of building heating or cooling using the soil as heat reservoir. *Int J Heat Mass Transf* 2006;49(21–22):4152–60.
- [7] Bourret B, Javelas R. Simulation of an underground solar energy storage for a dwelling. *Sol Energy* 1991;47(4):307–10.
- [8] Schmidt T, Mangold D, Müller-Steinhagen H. Central solar heating plants with seasonal storage in Germany. *Sol Energy* 2004;76(1–3):165–74.
- [9] Sweet ML, McLeskey Jr JT. Numerical simulation of underground Seasonal Solar Thermal Energy Storage (SSTES) for a single family dwelling using TRNSYS. *Sol Energy* 2012;86(1):289–300.
- [10] Yumrutaş R, Ünsal M. Energy analysis and modeling of a solar assisted house heating system with a heat pump and an underground energy storage tank. *Sol Energy* 2012;86(3):983–93.
- [11] Shelton J. Underground storage of heat in solar heating systems. *Sol Energy* 1975;17(2):137–43.
- [12] Givoni B. Underground longterm storage of solar energy—an overview. *Sol Energy* 1977;19(6):617–23.
- [13] Reuss M, Beck M, Müller JP. Design of a seasonal thermal energy storage in the ground. *Sol Energy* 1997;59(4–6):247–57.
- [14] Bertermann D, Klug H, Morper-Busch L. A pan-European planning basis for estimating the very shallow geothermal energy potentials. *Int J Renew Energy*;x(x):xx–xx, submitted for publication.
- [15] Directive. Directive 2009/28/EC of the European Parliament and of the Council of 23 April 2009 on the promotion of the use of energy from renewable sources and amending and subsequently repealing Directives 2001/77/EC and 2003/30/EC (Text with EEA relevance). 2009/28/EC.
- [16] Wu SH, Jansson PE, Zhang XY. Modelling temperature, moisture and surface heat balance in bare soil under seasonal frost conditions in China. *Eur J Soil Sci* 2011;62(6):780–96.
- [17] Lipiec J, Usowicz B, Ferrero A. Impact of soil compaction and wetness on thermal properties of sloping vineyard soil. *Int J Heat Mass Transf* 2007;50(19–20):3837–47.

- [18] Usovicz B, Lipiec J, Ferrero A. Prediction of soil thermal conductivity based on penetration resistance and water content or air-filled porosity. *Int J Heat Mass Transf* 2006;49(25–26):5010–7.
- [19] Ochsner TE, Horton R, Ren T. A new perspective on soil thermal properties. *Journal Paper No. J-19021 of the Iowa Agriculture and Home Economics Experiment Station, Ames, IA, Project No. 3287. Supported by the Hatch Act and the State of Iowa. Soil Sci Soc Am J* 2001;65(6):1641–7.
- [20] Yun TS, Santamarina JC. Fundamental study of thermal conduction in dry soils. *Granul Matter* 2008;10(3):197–207.
- [21] Usovicz B, Kossowski J, Baranowski P. Spatial variability of soil thermal properties in cultivated fields. *Soil Tillage Res* 1996;39(1–2):85–100.
- [22] Besson A, Cousin I, Bourennane H, Nicoulaud B, Pasquier C, Richard G, et al. The spatial and temporal organization of soil water at the field scale as described by electrical resistivity measurements. *Eur J Soil Sci* 2010;61(1):120–32.
- [23] Vogel HJ, Weller U, Schlüter S. Quantification of soil structure based on Minkowski functions. *Comput Geosci* 2010;36(10):1236–45.
- [24] de la Rosa D, Mayol F, Moreno F, Cabrera F, Díaz-Pereira E, Antoine J. A multilingual soil profile database (SDBm Plus) as an essential part of land resources information systems. *J Environ Model Softw* 2002;17(8):721–30.
- [25] Panagos P, Van Liedekerke M, Jones A, Montanarella L. European Soil Data Centre: response to European policy support and public data requirements. *Land Use Policy* 2012;29(2):329–38.
- [26] Goovaerts P. A coherent geostatistical approach for combining choropleth map and field data in the spatial interpolation of soil properties. *Eur J Soil Sci* 2011;62(3):371–80.
- [27] Ahangar-Asr A, Faramarzi A, Mottaghifard N, Javadi AA. Modeling of permeability and compaction characteristics of soils using evolutionary polynomial regression. *Comput Geosci* 2011;37(11):1860–9.
- [28] Monga O, Bouso M, Garnier P, Pot V. Using pore space 3D geometrical modelling to simulate biological activity: impact of soil structure. *Comput Geosci* 2009;35(9):1789–801.
- [29] Brus DJ, Kempen B, Heuvelink GBM. Sampling for validation of digital soil maps. *Eur J Soil Sci* 2011;62(3):394–407.
- [30] Moreira CS, Brunet D, Verneyre L, Sá SMO, Galdos MV, Cerri CC, et al. Near infrared spectroscopy for soil bulk density assessment. *Eur J Soil Sci* 2009;60(5):785–91.
- [31] Touma J. Comparison of the soil hydraulic conductivity predicted from its water retention expressed by the equation of Van Genuchten and different capillary models. *Eur J Soil Sci* 2009;60(4):671–80.
- [32] Hiraiwa Y, Kasubuchi T. Temperature dependence of thermal conductivity of soil over a wide range of temperature (5–75 °C). *Eur J Soil Sci* 2000;51(2):211–8.
- [33] Florides GA, Pouloupatis PD, Kalogirou S, Messaritis V, Panayides I, Zomeni Z, et al. The geothermal characteristics of the ground and the potential of using ground coupled heat pumps in Cyprus. *Energy* 2011;36(8):5027–36.
- [34] Schreiber D. Entwurf einer Klimaeinteilung für landwirtschaftliche Belange. Paderborn: Bochumer Geographische Arbeiten; 1973.
- [35] Dinku T, Connor SJ, Ceccato P, Ropelewski CF. Comparison of global gridded precipitation products over a mountainous region of Africa. *Int J Climatol* 2008;28(12):1627–38.
- [36] Museum of Vertebrate Zoology. WorldClim. Monthly precipitation and mean and min temperature data for current conditions (~1950–2000). Interpolated data of global weather stations. Berkeley University of California; 2012.
- [37] Frei C, Schöll R, Fukutome S, Schmidli J, Vidale PL. Future change of precipitation extremes in Europe: intercomparison of scenarios from regional climate models. *J Geophys Res* 2006;111(D6):D06105.
- [38] Baggs SA. Remote prediction of ground temperature in Australian soils and mapping its distribution. *Sol Energy* 1983;30(4):351–66.
- [39] Moustafa S, Jarrar D, el-Mansy H, Al-Shami H, Brusewitz G. Arid soil temperature model. *Sol Energy* 1981;27(1):83–8.
- [40] Mihalakakou G. On estimating soil surface temperature profiles. *Energy Build* 2002;34(3):251–9.
- [41] Kettridge N, Baird A. Modelling soil temperatures in northern peatlands. *Eur J Soil Sci* 2008;59(2):327–38.
- [42] Zhang J, Wang Y, Li Y. A C++ program for retrieving land surface temperature from the data of Landsat TM/ETM+ band6. *Comput Geosci* 2006;32(10):1796–805.
- [43] Balghouthi M, Kooli S, Farhat A, Daghari H, Belghith A. Experimental investigation of thermal and moisture behaviors of wet and dry soils with buried capillary heating system. *Sol Energy* 2005;79(6):669–81.
- [44] Harris G. Integrated assessment and modelling: an essential way of doing science. *J Environ Model Softw* 2002;17(3):201–7.
- [45] Friedler F. Process integration, modelling and optimisation for energy saving and pollution reduction. *Appl Therm Eng* 2010;30(16):2270–80.
- [46] IUSS Working Group WRB. World reference base for soil resources 2006. Rome: FAO; 2006.
- [47] Kersten MS. Thermal properties of soils. *Bulletin* 28, LII/21. Minnesota: University of Minnesota; 1949.
- [48] Dehner U. Bestimmung der thermischen Eigenschaften von Böden als Grundlage für die Erdwärmenutzung. *Mainz Geowiss Mittl* 2007;35:159–86.
- [49] Berry W, Ketterings Q, Antes S, Page S, Russell-Anelli J, Rao R, et al. Soil texture. *Agron Fact Sheet Ser* 2007;29:1–2.
- [50] Ad-hoc-AG-Boden. Bodenkundliche Kartieranleitung, KA5. Hannover: Schweizerbart'sche Verlagsbuchhandlung; 2005.
- [51] Kuntze H, Roeschmann G, Schwerdtfeger G. *Bodenkunde*. Stuttgart: Eugen Ulmer; 1994.
- [52] Usovicz B, Lipiec J, Usovicz JB. Thermal conductivity in relation to porosity and hardness of terrestrial porous media. *Planet Space Sci* 2008;56(3–4):438–47.
- [53] DIN 18121. Baugrund, Untersuchung von Bodenproben – Wassergehalt – Teil 2: Bestimmung durch Schnellverfahren [Soil, investigation and testing – water content – Part 2: Determination by rapid methods]; 2012.
- [54] DIN 18126. Baugrund, Untersuchung von Bodenproben – Bestimmung der Dichte nichtbindiger Böden bei lockerster und dichtester Lagerung [Soil, investigation and testing – determination of density of non-cohesive soils for maximum and minimum compactness]; 1996.
- [55] Webb PA. The SediGraph method of particle sizing. In: *Micromeritics*. Micromeritics; 2004.
- [56] TeKa. TK04-sample preparation: instructions for preparing samples for TK04 laboratory tests. Berlin: TeKa; 2009. <http://www.te-ka.de/en/pdf/TK04-SamplePreparation.pdf>.
- [57] ISO 19128. Geographic information – web map server interface; 2005. p. 76.
- [58] OGC. Styled layer descriptor profile of the web map service implementation specification, 2007-06-29, OGC 05-078r4, version: 1.1.0, Dr. Markus Lupp. SLD 110. The Open Geospatial Consortium (OGC); 2007. <http://www.opengeospatial.org/standards/sls>.
- [59] Yoon G, Tanaka H, Okumiya M. Study on the design procedure for a multi-cool/heat tube system. *Sol Energy* 2009;83(8):1415–24.
- [60] Benli H, Durmuş A. Evaluation of ground-source heat pump combined latent heat storage system performance in greenhouse heating. *Energy Build* 2009;41(2):220–8.
- [61] Haehnlein S, Bayer P, Blum P. International legal status of the use of shallow geothermal energy. *Renew Sustain Energy Rev* 2010;14(9):2611–25.
- [62] Bernard L, Kanellopoulos I, Annoni A, Smits P. The European geoportal—one step towards the establishment of a European Spatial Data Infrastructure. *Comput Environ Urban Syst* 2005;29(1):15–31.
- [63] Klug H, Bretz B. Discover INSPIRE compliant harmonised soil data and services. Final product summary of the GS Soil Project on “Assessment and strategic development of INSPIRE compliant Geodata-Services for European Soil Data”. Salzburg: Co-funded by the Community Programme eContentplus ECP_2008_GEO_318004; 2012. p. 60.
- [64] Minasny B, Mc Bratney AB. Uncertainty analysis for pedotransfer functions. *Eur J Soil Sci* 2002;53(3):417–29.
- [65] Pachepsky YA, Rawls WJ. Soil structure and pedotransfer functions. *Eur J Soil Sci* 2003;54(3):443–52.
- [66] Hwang SI, Yun EY, Ro HM. Estimation of soil water retention function based on asymmetry between particle- and pore-size distributions. *Eur J Soil Sci* 2011;62(2):195–205.
- [67] Vdović N, Obhodaš J, Pikelj K. Revisiting the particle-size distribution of soils: comparison of different methods and sample pre-treatments. *Eur J Soil Sci* 2010;61(6):854–64.
- [68] Carrick S, Almond P, Buchan G, Smith N. In situ characterization of hydraulic conductivities of individual soil profile layers during infiltration over long time periods. *Eur J Soil Sci* 2010;61(6):1056–69.
- [69] Hu W, Shao MA, Si BC. Seasonal changes in surface bulk density and saturated hydraulic conductivity of natural landscapes. *Eur J Soil Sci* 2012;63(6):820–30.
- [70] Momose T, Kasubuchi T. Effect of reduced air pressure on soil thermal conductivity over a wide range of water content and temperature. *Eur J Soil Sci* 2002;53(4):599–606.
- [71] Coutadeur C, Coquet Y, Roger-Estrade J. Variation of hydraulic conductivity in a tilled soil. *Eur J Soil Sci* 2002;53(4):619–28.
- [72] Kroll JA, Ziegler F. The use of ground heat storages and evacuated tube solar collectors for meeting the annual heating demand of family-sized houses. *Sol Energy* 2011;85(11):2611–21.